

Article

Immobilization of Lipases on Modified Silica Clay for Bio-Diesel Production: The Effect of Surface Hydrophobicity on Performance

Youdan Duan ^{1,2}, Ting Zou ¹, Sijin Wu ¹ and Haiming Cheng ^{1,2,*} 

¹ The Key Laboratory of Leather Chemistry and Engineering of Ministry of Education, Sichuan University, Chengdu 610065, China; 2019223080039@stu.scu.edu.cn (Y.D.); 2018223080014@stu.scu.edu.cn (T.Z.); gary_dunphy@163.com (S.W.)

² National Engineering Laboratory for Clean Technology of Leather Manufacture, Sichuan University, Chengdu 610065, China

* Correspondence: chenghaiming@scu.edu.cn

Abstract: The hydrophobicity of a support plays a critical role in the catalytic efficiency of immobilized lipases. 3-aminopropyltriethoxysilane (APTES)-modified silica clay (A-SC) was coupled with silane coupling agents of different alkyl chains (methyl triethoxysilane, vinyl triethoxysilane, octyl triethoxysilane, and dodecyl triethoxysilane) to prepare a series of hydrophobic support for lipase immobilization. The lipases were immobilized onto the support by conducting glutaraldehyde cross-linking processes. The results showed that the activity of the immobilized biocatalyst increased with hydrophobicity. The hydrolytic activity of Lip-Glu-C₁₂-SC (contact angle 119.8°) can reach 5900 U/g, which was about three times that of Lip-Glu-A-SC (contact angle 46.5°). The immobilized lipase was applied as a biocatalyst for biodiesel production. The results showed that the catalytic yield of biodiesel with highly hydrophobic Lip-Glu-C₁₂-SC could be as high as 96%, which is about 30% higher than that of Lip-Glu-A-SC. After being recycled five times, the immobilized lipase still maintained good catalytic activity and stability. This study provides a good strategy to improve the efficiency of immobilized lipases, showing great potential for future industrial application on biodiesel production.

Keywords: lipase; silica; biodiesel; immobilization; hydrophobic modification



Citation: Duan, Y.; Zou, T.; Wu, S.; Cheng, H. Immobilization of Lipases on Modified Silica Clay for Bio-Diesel Production: The Effect of Surface Hydrophobicity on Performance. *Catalysts* **2022**, *12*, 242. <https://doi.org/10.3390/catal12020242>

Academic Editors: Vincenzo Vaiano and Olga Sacco

Received: 19 January 2022

Accepted: 17 February 2022

Published: 21 February 2022

Publisher's Note: MDPI stays neutral with regard to jurisdictional claims in published maps and institutional affiliations.



Copyright: © 2022 by the authors. Licensee MDPI, Basel, Switzerland. This article is an open access article distributed under the terms and conditions of the Creative Commons Attribution (CC BY) license (<https://creativecommons.org/licenses/by/4.0/>).

1. Introduction

Lipases (triacylglycerol hydrolase, E.C. 3.1.1.3) catalyze reactions such as the hydrolysis of triacylglycerol, esterification, transesterification, and interesterification. They present high activity, good stability, unique selectivity, and specificity. Therefore, they have been widely used in many fields of biotechnology and bioengineering [1–5]. In order to enhance its stability and reusability, lipases can be immobilized on various supports by techniques such as physical adsorption, embedding, covalent binding, and cross-linking [6–9]. These immobilization methods can perform the recovery and reuse of biocatalysts, control the loss of enzymes, reduce process costs, and improve its feasibility [10].

The catalytic active site of lipase is comprises a catalytic triad (Ser-His-Asp/Glu), oxygen anion pore and hydrophobic cavity, and the surface is covered by a relatively hydrophobic amphiphilic α -helical polypeptide chains (also known as “lid”), which protect the active site of the triad [11]. The outer surface of the “lid” is relatively hydrophilic, while the inner surface is relatively hydrophobic [1]. While the hydrophobic interface exists, the “lid” moves, and the α -helix is reoriented to expose the active center [4]; thus, the lipase is fixed and adsorbed on the hydrophobic surface in an open form and maintains high activity [12]. Due to the hydrophobic interaction between the hydrophobic surface and the lipase, the enzyme can be activated from an inactive (closed cap) state to an active (open cap)

state, which is called “interface activation” [13–18]. Moreover, the combination of lipase and a hydrophobic surface is very strong and occurs quickly [4]. The hydrophobic interface reduces hydrogen bond interactions between lipase and water, and the enzyme forms an incomplete hydration layer, while the aliphatic sidechains of hydrophobic substrates fold onto the surface of enzyme molecules to maintain open conformation, and it improves the catalytic efficiency of enzyme reaction [1]. “Interface activation” has been applied to control the conformation of lipase active sites by regulating supports with different degrees of hydrophobicity [10], such as magnetic grapheme oxide [6], silica nanotubes [19], and polylactic acid scaffolds [20], which were modified to obtain high surface hydrophobicity and used as the immobilization support for lipases. The immobilizations of the lipase on the hydrophobic support usually occur via interfacial activation [19–21]. However, the enzymes immobilized by this protocol might be released to the medium under certain conditions [21], such as high temperature, organic cosolvents, and ionic strength environments [22–25]. It can decrease the activation of the enzyme and contaminate the product. Therefore, the development of stable and suitable hydrophobic supports for immobilization of lipases needs further exploration.

In our previous study, the cheap and easily obtained silica clay showed good performance as lipase immobilization support for biodiesel production [26]. Herein, a series of silica coupling agents with various lengths of alkyl chain was coupled with silica clay for the synthesis of a series of novel alkyl-modified silica clay support to impart the support with different degrees of hydrophobicity. Moreover, lipase protein molecules were immobilized onto the support by cross-linking via glutaraldehyde. The effects of hydrophobicity of the support surface on the properties of the immobilized lipase and its performance on biodiesel production were investigated.

2. Results and Discussion

2.1. Characterization

Fourier transform infrared (FT-IR) profiles of the silica clay supports are shown in Figure 1A. There were characteristic peaks at 1100 and 810 cm^{-1} , which can be attributed to the vibration of Si-O-Si [27]. The absorption peaks at 2880 and 2964 cm^{-1} can be attributed to the stretching vibration of the C-H bond in the modified alkyl group, while the peaks at 1450 and 1500 cm^{-1} can be attributed to the bending vibration of C-H bonds in the alkyl group [28,29]. The results showed that the alkyl groups have been successfully introduced onto the silica clay.

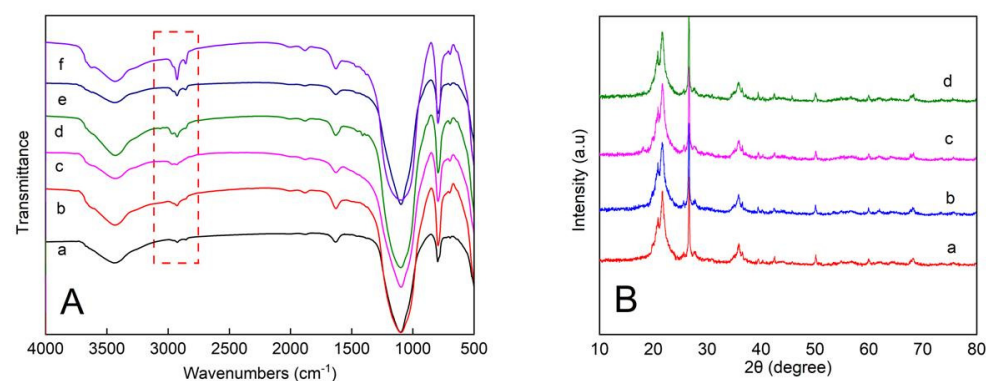


Figure 1. (A) FT-IR spectra of (a) SC, (b) A-SC, (c) CH_3 -SC, (d) $\text{CH}_2=\text{CH}_2$ -SC, (e) C_8 -SC, and (f) C_{12} -SC. (B) XRD patterns of (a) CH_3 -SC, (b) $\text{CH}_2=\text{CH}_2$ -SC, (c) C_8 -SC, and (d) C_{12} -SC.

The XRD patterns of CH_3 -SC, $\text{CH}_2=\text{CH}_2$ -SC, C_8 -SC, and C_{12} -SC are shown in Figure 1B. The main component of SC is amorphous silica material, which has characteristic broad peaks in the range of $2\theta = 15\text{--}30^\circ$ [30,31]. The patterns had a wide peak at $2\theta = 21.65^\circ$, confirming the successful synthesis of CH_3 -SC, $\text{CH}_2=\text{CH}_2$ -SC, C_8 -SC, and C_{12} -SC. XRD results illustrate that different hydrophobic degree modifications do not cause changes

to SC structure. Furthermore, the elemental compositions of N, H, C, and S in CH₃-SC, CH₂=CH₂-SC, C₈-SC, and C₁₂-SC are shown in Table 1. According to the different lengths of alkyl, the content of C and H elements increased with increases in the alkyl chain. These results indicated that CH₃-SC, CH₂=CH₂-SC, C₈-SC, and C₁₂-SC could be introduced onto silica clay supports for enzyme immobilization. Furthermore, SEM images show that CH₃-SC, CH₂=CH₂-SC, C₈-SC, and C₁₂-SC maintained typical irregular flake structures of SC (Figure 2). There is no obvious difference in surface morphologies after modification, illustrating that the modification process with various alkyl chains of silane coupling agents did not change the surface morphology of SC.

Table 1. The elemental composition of the samples.

Samples	N (%)	C (%)	H (%)	S (%)
CH ₃ -SC	0.42	2.47	0.94	0
CH ₂ =CH ₂ -SC	0.39	3.12	0.98	0
C ₈ -SC	0.40	3.22	1.11	0
C ₁₂ -SC	0.42	3.71	1.09	0

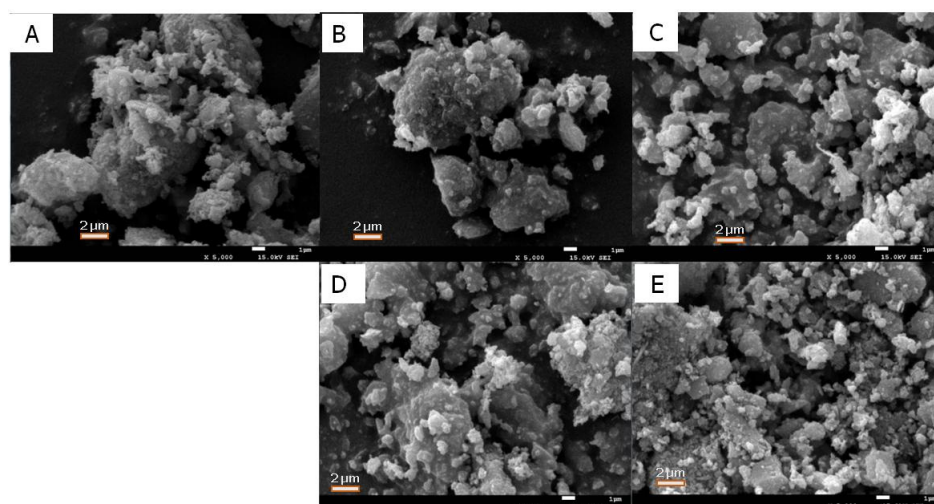


Figure 2. SEM images. (A) A-SC, (B) CH₃-SC, (C) CH₂=CH₂-SC, (D) C₈-SC, and (E) C₁₂-SC.

The hydrophobicities of A-SC after hydrophobic modification and enzymatic immobilization were tested by using contact angle measurements (Figure 3). The contact angle reflected the hydrophobicity of the material. A high degree of the contact angle means good hydrophobicity [10]. The results show that the contact angles of A-SC and Lip-Glu-A-SC are 64.3° and 46.5°, respectively (Table 2, Figure 3). With the modification of methyl, vinyl, octyl, and dodecyl, the degree of the CA of the SC support increased to 119.5°, 122.1°, 132.1°, and 142.3°, respectively, indicating an increase in hydrophobicity [11]. However, after immobilization with lipase, their contact angles decreased (Table 2, Figure 3). The contact angles of Lip-Glu-CH₃-SC, Lip-Glu-CH₂=CH₂-SC, Lip-Glu-C₈-SC, and Lip-Glu-C₁₂-SC were 97.7°, 101.3°, 112.5°, and 119.8°, respectively (Figure 3). This may be due to the binding of the hydrophilic enzyme molecules onto the support.

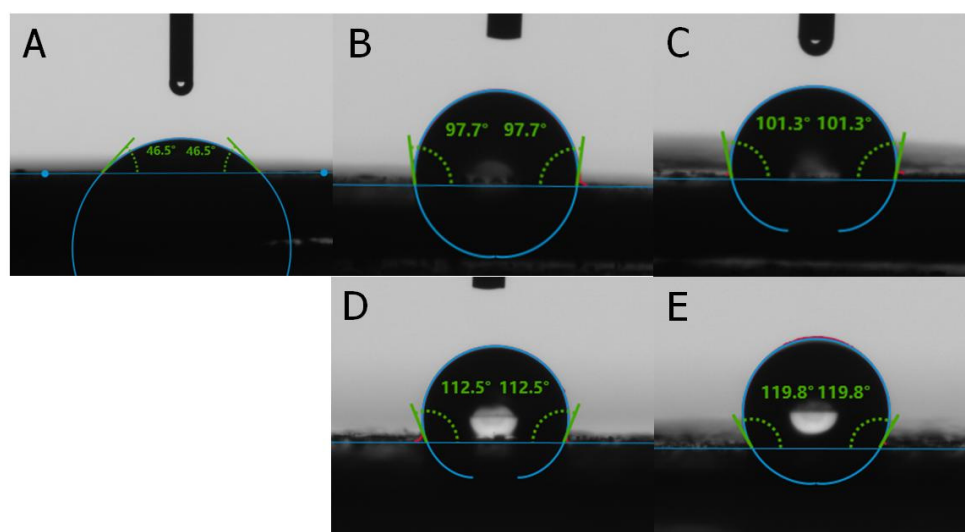


Figure 3. Contact angle of immobilized samples. (A) Lip-Glu-A-SC, (B) Lip-Glu-CH₃-SC, (C) Lip-Glu-CH₂=CH₂-SC, (D) Lip-Glu-C₈-SC, and (E) Lip-Glu-C₁₂-SC.

Table 2. The contact angle of support modified by silane coupling agents.

Samples	A-SC	CH ₃ -SC	CH ₂ =CH ₂ -SC	C ₈ -SC	C ₁₂ -SC
Contact angle (°)	64.3	119.5	122.1	132.1	143.2

2.2. Loading Efficiency and Hydrolytic Activity of Immobilized Enzyme

2.2.1. Loading Efficiency of Immobilization

The effects of surface hydrophobicity of the support on the loading efficiency of lipase is shown in Figure 4. The results showed that with the increase in hydrophobicity, the loading efficiency of lipase on the support increases slightly, with no notable change on loading efficiencies. It could be because the immobilization of lipase was mainly achieved through the covalent cross-linking of glutaraldehyde [32].

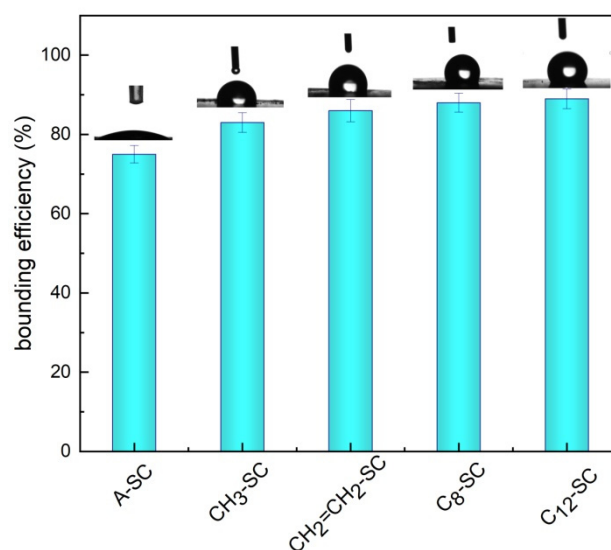


Figure 4. The bounding efficiency of lipase onto various hydrophobic supports.

2.2.2. Hydrolytic Activity of Immobilized Enzyme

The effects of surface hydrophobicity of the support on the hydrolytic activity of the immobilized lipase is shown in Figure 5. It could be observed that the hydrolytic activity of the immobilized enzyme increased with the increase in hydrophobicity of the

support. The hydrolytic activity of Lip-Glu-C₁₂-SC (CA 119.8°) reached 5900 u/g, while the activity of Lip-Glu-A-SC (CA 46.5°) was 2000 u/g. The tremendous increase in activity suggests that the existence of hydrophobic groups might activate the active center of lipase molecules, opening the “lid” structure at the center, which results in the entry of substrate molecules easily [33]. Similar results were reported by the immobilization of lipases on alkyl silane-modified magnetic nanoparticles [29] and on divinylsulfone-activated agarose [34].

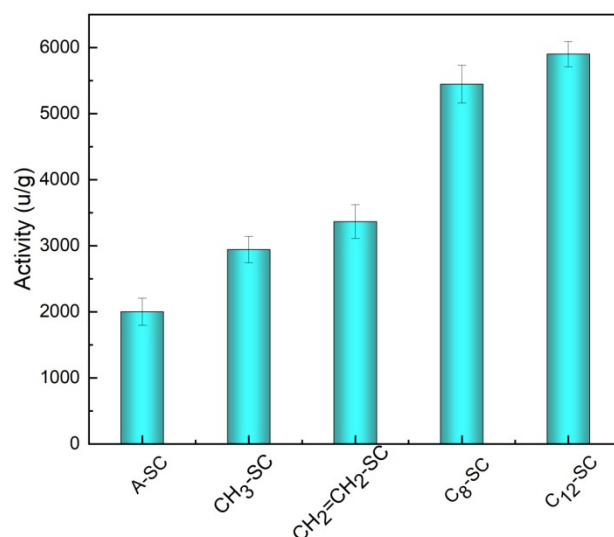


Figure 5. The hydrolytic activity of immobilized lipase onto hydrophobic supports.

2.3. Enzymatic Properties of Immobilized Lipase

2.3.1. Effect of Temperature

The effect of temperature on the hydrolytic activity of free enzymes, Lip-Glu-A-SC (CA 46.5°) and Lip-Glu-C₁₂-SC (CA 119.8°), was investigated at pH 7.5 by varying the temperature from 20 to 70 °C (Figure 6A). The results showed that the temperature corresponding to the maximum activity of the free enzyme and the two types of immobilized lipase were 50 °C. The optimum temperature range of two types of immobilized lipase was wider than that of the free enzyme and could maintain more than 90% of enzyme activity in the temperature range of 40–70 °C. However, with further increases in temperature, the free enzyme was seriously inactivated, which may be caused by the conformational change of free enzyme activity in higher temperatures. The enzyme immobilized on the hydrophobic support was less sensitive to temperature and retained high activity under high temperatures. It is possible that the formation of multipoint hydrophobic interactions between the alkyl group and enzyme molecule made the enzyme molecular structure more rigid and avoided a distortion of enzyme structure [15].

2.3.2. Effect of pH

The effect of pH on enzyme activity was investigated at 40 °C by varying the pH from 4 to 9 (Figure 6B). Figure 6B showed that the optimal pH of the two immobilized enzymes was at 8.0, which was one unit shifted from the optimal pH 7.0 of the free enzyme. This shift may be due to the accumulation of fatty acids produced during hydrolysis near the catalytic region of the immobilized enzyme, which decreased the pH of the catalytic microenvironment. Therefore, the optimal pH of the immobilized enzymes could be achieved by appropriately increasing pH [35]. Moreover, the immobilized enzyme showed less sensitivity to pH; Lip-Glu-C₁₂-SC could maintain 80% enzyme activity under pH 4.0, which was much higher than that of the free enzyme (55%) and Lip-Glu-A-SC (70%). The higher enzyme activity could be due to hydrophobic interactions enhancing molecular rigidity and stabilizing the active conformation of enzyme molecules; thus, the immobilized enzyme could better adapt to more complex reaction systems [21].

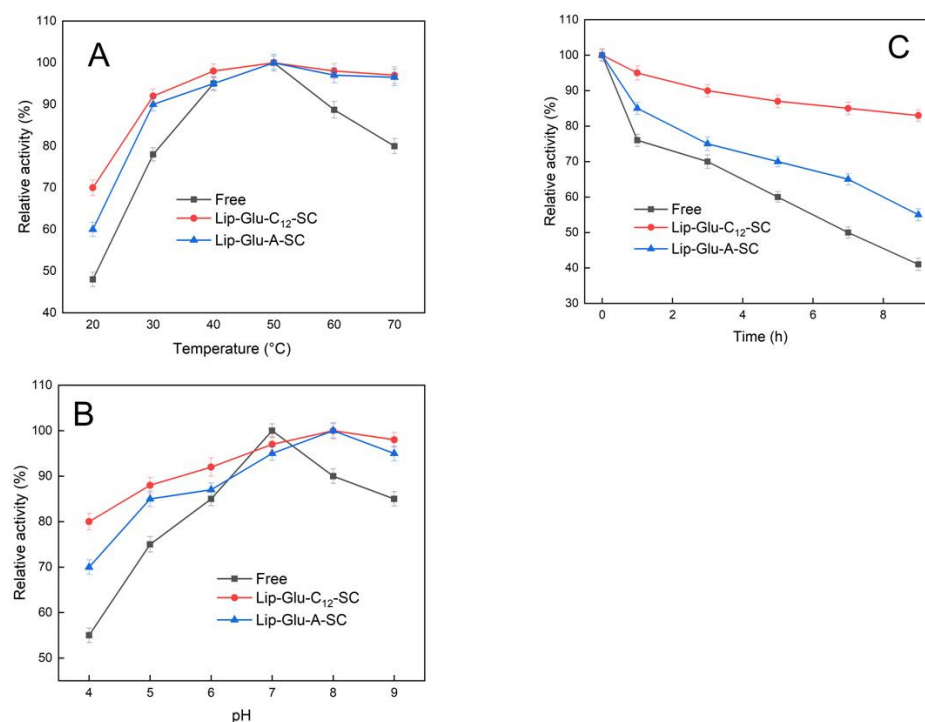


Figure 6. Effect of temperature (A); effect of pH (B); thermal stability (C).

2.3.3. Effect on Thermal Stability

The thermal stability of the free and immobilized enzyme was measured by testing its hydrolytic activity at pH 7.5 and 60 °C by varying the incubation duration. The relative activity was set at 100% at the beginning of the incubation. It could be observed from Figure 6C that after 9 h of incubation, the relative activity of the free lipase was only maintained around 40%, while the relative activity of Lip-Glu-A-SC and Lip-Glu-C₁₂-SC could be kept at 57% and 87%, respectively. This illustrates that the thermal stability of the lipase after immobilization significantly improved. Furthermore, the higher the hydrophobic degree of immobilized lipase, the higher the thermal stability will be. This may be due to the hydrophobic interaction contributing to the maintenance of stable conformation of the enzyme, which was consistent with other reports [2,34,36].

2.4. Biodiesel Synthesis

The effect of immobilized lipase with different hydrophobic degrees on the conversion yield of biodiesel was investigated (Figure 7). The conversion yield of biodiesel increased with the increase on hydrophobicity of the support. Lip-Glu-C₁₂-SC with the highest hydrophobic degree had the highest conversion yield, reaching 96.7%, while the catalytic conversion yield of Lip-Glu-A-SC was only 70%. The high conversion yield was at a similar level, as previously reported [37]. This result implies that the local hydrophobic interaction between alkyl and lipase molecules activated the active conformation of lipase. The enhanced hydrophobic interaction on the surface of the carrier enlarged the opening range of the “lid” structure of the active lipase region, and the accessibility of the lipid substrate to the active site was stronger [21]. Furthermore, the hydrophobic support was more conducive to enriching hydrophobic substrates; thus, the hydrophobic support might prevent the inhibitory effect of glycerol. This may also be one of the reasons for the improvement of its catalytic activity [38–40]. In order to further verify the effects of surface hydrophobicity of the support on the yield of biodiesel, the immobilized lipase was incubated in dimethyl sulfoxide (DMSO) and water (*v/v* 1:1) before being added into the reaction system. Figure 7 shows that yield decreased dramatically while the immobilized lipase incubated with water. The results reveal that the hydrophobic microenvironment on the surface of immobilized lipase was destroyed by the presence of water, which reduces

local hydrophobic interactions, in turn intensely affecting the catalytic efficiency of the immobilized lipase.

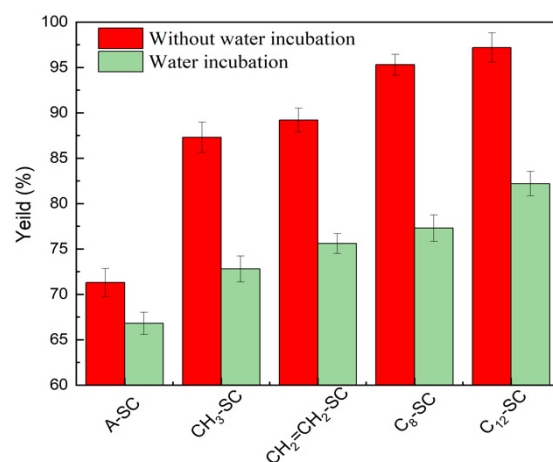


Figure 7. Effect of immobilized lipase with different hydrophobicity on biodiesel yield.

The properties of the prepared product were tested according to the Chinese National Standard GB/T 2013-2010, GB/T 265-1988, GB 264-1983, and GB/T 17144-1997. [40–43] (Table 3). The results showed that the physical and chemical indicators of biodiesel were all within the range of the standard. It indicated that the prepared product could be used as biodiesel.

Table 3. The properties of biodiesel catalyzed by Lip-Glu-C₁₂-SC.

Property	Result	Standard Range	Standard/ Method
Density (20 °C /kg m ⁻³)	873	820–900	GB/T 2013-2010/ Densimeter
Kinematic viscosity (40 °C /mm ² s ⁻¹)	4.5	1.9–6.0	GB/T 265-1988/ Capillary viscometer
Acid value (mg KOH g ⁻¹)	0.10	≤0.8	GB 264-1983/ KOH titration
Residual carbon content (%)	0.03	<0.3	GB/T 17144-1997/ Muffle furnace

Waste cooking oil (acid value (KOH) 4.2 mg/g, saponification value (KOH) 179.3 mg/g, density 0.875 g/cm³) obtained from local market was spun at 10,000 rpm for 10 min. Then, it was applied for the production of biodiesel by the prepared immobilized lipase. The results showed that conversion yields could reach 92.3% for Lip-Glu-C₁₂-SC. It revealed that the prepared immobilized lipases showed a good prospect for industrial applications of biodiesel production.

2.5. Reusability of Immobilized Lipase

The reusability of immobilized lipase with different hydrophobicities in the synthesis of biodiesel was investigated. With the increase in immobilized enzyme use, the efficiency of catalytic synthesis of biodiesel decreased gradually (Figure 8). After being used more than five times, the immobilized enzymes on the hydrophobic supports still retained high conversion rates (above 85%), indicating that the hydrophobic support had a good advantage in the maintenance of immobilized enzyme activity and stability. The reusability is better than that of adsorption immobilization methods [29,37]. The decreasing conversion rate of catalytic biodiesel may be due to the destruction of enzyme molecules by temperature and the partial loss of immobilized enzymes caused by the repeatability of operations.

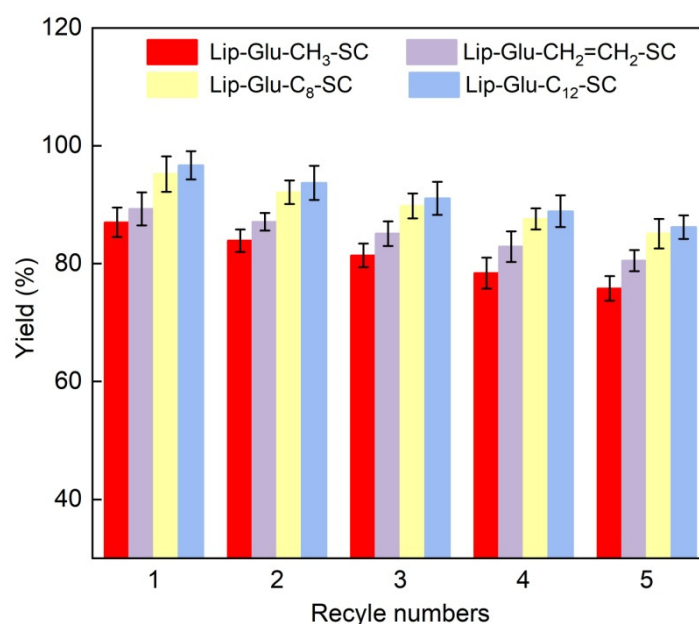


Figure 8. Reusability of immobilized lipases with hydrophobic modification.

3. Materials and Methods

3.1. Materials

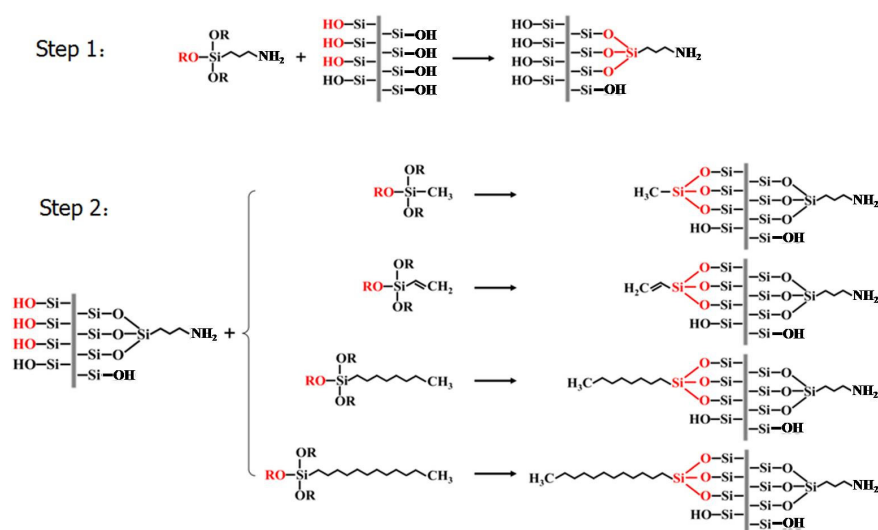
Lipase Eversa Transform 2.0 was obtained from Novozymes China (Beijing, China). Silicon Clay (SC) was obtained from Ningbo Create New Materials Co, (Ningbo, China). 3-aminopropyltriethoxysilane (APTES) and *n*-hexane (chromatographic grade) were purchased from Aladdin (Shanghai, China). Methyl heptadecanoate was purchased from Sigma-Aldrich (Shanghai, China). Methyltriethoxysilane and Octyltriethoxysilane were purchased from Jiuding Chemical Co (Shanghai, China). Vinyltriethoxysilane and Dodecyltriethoxysilane were purchased from Aladdin (Shanghai, China). Rapeseed oil (fat 99.9%, free fatty acid 0%, protein 0%, and water 0%) and olive oil were purchased from a local market (Chengdu, China). All other reagents are analytical grade reagents and can be used without further purification.

3.2. Preparation of Hydrophobic Silica Clay and Immobilization of Lipase

3.2.1. Hydrophobic Modification on Silica Clay

Step 1: Silica clay measuring 4.0 g was dispersed in 30 mL of anhydrous ethanol for 30 min using ultrasonication. Then, 5.0 mL of 3-aminopropyltriethoxysilane (APTES) was added into the mixture, which was heated at 80 °C with refluxing for 24 h under nitrogen atmosphere with gentle magnetic stirring. After the reaction finished, the mixture was washed with anhydrous ethanol several times to remove excess APTES, and then it was desiccated at 60 °C. APTES-modified SC was designated as A-SC.

Step 2: The obtained A-SC was dispersed with 30 mL of toluene, and then 3.0 mL of silane coupling agents was added. The mixture was refluxed in a nitrogen atmosphere for 24 h. After the reaction, the excess silane coupling agent was washed with toluene and anhydrous ethanol and then dried to constant weight at 60 °C. The schematic diagram of the preparation is shown in Scheme 1. Modified A-SCs by different coupling agents are assigned as follows: CH₃-SC (methyl triethoxysilane), CH₂=CH₂-SC (vinyl triethoxysilane), C₈-SC (octyl triethoxysilane), and C₁₂-SC (dodecyl triethoxysilane).



Scheme 1. The preparation of hydrophobic silica clay supports.

3.2.2. Immobilization of Lipase

Glutaraldehyde-activated supports and its immobilization process with lipase were described in our previous report [26]. Briefly, 1.0 g of the modified silica clay was dispersed in 10 mL of glutaraldehyde solution at 30 °C for 2 h with gentle shaking. After that, it was washed thoroughly with sodium phosphate buffer (pH 7.5) to obtain glutaraldehyde-activated silica clay. For immobilization with lipase, 1.0 g of support was mixed with 10 mL of 0.1 mol/L sodium phosphate buffer (pH 7.5) containing a set concentration of lipase solution at 30 °C for 60 min with constant stirring. Then, in order to remove the free lipase, the supports were washed several times with 0.1 mol/L sodium phosphate buffer (pH 7.5). The immobilized lipase was dried at 60 °C to a constant weight. The obtained immobilized lipases were designated as Lip-Glu-A-SC, Lip-Glu-CH₃-SC, Lip-Glu-CH₂=CH₂-SC, Lip-Glu-C₈-SC, and Lip-Glu-C₁₂-SC, respectively.

3.3. Characterization

The Fourier transform Infrared (FTIR) spectra of the samples were collected on a Nicolet Is10 infrared spectrometer (Thermo Fisher Scientific, Boston, MA, USA) by the KBr pellet method over a range from 4000 to 400 cm⁻¹. X-ray diffraction profiles were obtained from an X'Pert Pro MPD DY 129 X-ray diffractometer (Oxford Instruments, UK). The morphologies of the modified silica support were observed by a FEI XL-30 scanning electron microscope (SEM) (FEI, Hillsboro, OR, USA). The elemental composition (C, H, N, and S) of each sample was determined by a Flash-Smart NCS element analyzer (Thermo Fisher Scientific, USA). The contact angle (CA) of the samples was measured by a HARKE-SPCAX3 contact angle tester (Dataphysics Instruments, Germany).

3.4. Determination of Immobilized Enzyme Loading

The protein content in the solution before and after immobilization was determined by using the Lowry assay [44]. Bovine serum albumin (BSA) was used as the standard protein. The loading efficiency of the support was calculated by Equation (1):

$$\text{Loading Efficiency mg/g} = \frac{(C_i - C_f)V}{W} \quad (1)$$

where C_i and C_f represent initial and final lipase protein concentrations in the immobilization process, V represents the solution volume, and W represents the weight of the support. All tests were conducted in triplicate.

3.5. Hydrolytic Activity Assay

The hydrolytic activities of lipases were evaluated by hydrolyzing olive oil emulsions containing 4% (*w/v*) of polyvinyl alcohol (PVA 1750). Briefly, the lipase sample was added to a mixture of 4 mL olive oil emulsion and 5 mL phosphate buffer (0.1 mol/L pH 7.5). The mixture was incubated at 40 °C for 15 min. Then, 15 mL of 95% ethanol was added to terminate the reaction and titration with 0.05 mol/L of sodium hydroxide solution was performed. One unit of lipase activity was defined as the amount of enzyme that liberated 1 μmol of free fatty acid per min under assay conditions. As the control, 15 mL of 95% ethanol was added before the addition of the enzyme.

3.6. Biodiesel Production

The immobilized lipases with various hydrophobic degrees were applied for biodiesel production. Briefly, 4.4 g of rapeseed oil, 5 mL of *n*-hexane as a cosolvent, and a set amount of immobilized lipase were mixed at 45 °C for 5 min. Then, methanol was added three times, with 0.16 g of methanol added dropwise each time. The reaction was carried out at 45 °C for 24 h. After the reaction, the immobilized catalyst was spun down and the supernatant was distilled under a vacuum to remove the solvent and excess methanol. The density, kinematic viscosity, acid value, and residual carbon content of the samples were determined according to the Chinese National Standards [40–43] GB/T 2013-2010, GB/T 265-1988, GB 264-1983, and GB/T 17144-1997, respectively. The content of fatty acid methyl ester in the product was determined by an Agilent 7890B gas chromatography analyzer (Agilent, Santa Clara, CA, USA) by using a hydrogen flame ion (FID) detector. The temperature of both the injection port and detector was set at 300 °C. The split ratio was 10:1, and the injection volume was 1.0 μL. The yield of biodiesel (%) was calculated by Equation (2):

$$\text{wt (\%)} = \frac{\sum A_i - A_{\text{MH}}}{A_{\text{MH}}} \times \frac{C_{\text{MH}} V_{\text{MH}} \times 100}{W} \quad (2)$$

where wt (%) is biodiesel yield, and $\sum A_i$ and A_{MH} represent the total peak area of fatty acid methyl ester and the peak area of methyl heptadecanoate, respectively. C_{MH} and V_{MH} represent the concentration and the volume of methyl heptadecanoate, and W is the weight of sample.

4. Conclusions

In conclusion, a series of APTES modified silica clay supports with different hydrophobicity for lipase immobilization was successfully prepared by reaction with silane coupling agents and glutaraldehyde cross-linking. The immobilized lipase was used as a biocatalyst for the production of biodiesel. We found that the tolerance of immobilized lipase to temperature and pH was improved dramatically while the support modified the hydrophobic alkyl chain. Meanwhile, the hydrolytic activity of lipase has been improved with the enhancement of the hydrophobicity of the support. The hydrolytic activity of Lip-Glu-C₁₂-SC (CA 119.8°) was 5900 u/g, which was about three-times higher than that of Lip-Glu-A-SC (CA 46.5°). Moreover, lipase immobilized on the hydrophobic surface of the support exhibited better biodiesel yield and reusability. The biodiesel yield of Lip-Glu-C₁₂-SC was 96.7%, which was 26.7% higher than that of Lip-Glu-A-SC. The relative activity still could be maintained at 85% after being recycled five times. The activity and stability of lipases immobilized on supports with hydrophobic alkyl chains were dramatically improved in comparison with supports without hydrophobic modification.

Author Contributions: Methodology, H.C., Y.D. and T.Z.; formal analysis, S.W.; investigation, Y.D., T.Z. and S.W.; writing—original draft preparation, Y.D. and T.Z.; writing—review and editing, H.C. All authors have read and agreed to the published version of the manuscript.

Funding: This research was funded by the National Key Technology R&D Program of China (No. 2017YFB0308400).

Data Availability Statement: Not applicable.

Acknowledgments: The authors thanks Xuekai Wang (Analytical & Testing Center, Sichuan University) for his help in GC detection.

Conflicts of Interest: The authors declare no conflict of interest.

References

1. Cheng, C.; Tian, Y.; Jiang, Y.L. Elucidation of lid open and orientation of lipase activated in interfacial activation by amphiphilic environment. *Inter. J. Biol. Macromol.* **2018**, *119*, 1211–1217. [[CrossRef](#)] [[PubMed](#)]
2. Sun, X.; Zhu, W.; Matyjaszewski, K. Protection of opening lids: Very high catalytic activity of lipase immobilized on core-shell nanoparticles. *Macromolecules* **2018**, *51*, 289–296. [[CrossRef](#)] [[PubMed](#)]
3. De, T.; Sikder, J.; Narayanan, C.M. Biodiesel synthesis using immobilised lipase enzyme in semi-fluidised bed bioreactors—bioreactor design and performance analysis. *Environ. Prog. Sustain. Energ.* **2017**, *36*, 1537–1545. [[CrossRef](#)]
4. Zhong, L.; Feng, Y.; Hu, H.; Xu, J. Enhanced enzymatic performance of immobilized lipase on metal organic frameworks with superhydrophobic coating for biodiesel production. *J. Colloid Interf. Sci.* **2021**, *602*, 426–436. [[CrossRef](#)] [[PubMed](#)]
5. Tacin, M.V.; Costa-Silva, T.A.; Paula, A.V. Microbial lipase: A new approach for a heterogeneous biocatalyst. *Prep. Biochem. Biotechnol.* **2021**, *51*, 749–760. [[CrossRef](#)] [[PubMed](#)]
6. Wang, Y.E.; Zhang, Z.A.; Tang, A.X. Modification of magnetic graphene oxide with covalent A to fix lipase CRL by surfactants. *Chem. Ind. Eng. Prog.* **2019**, *38*, 4255–4263.
7. Ying, M.; Chen, G. Study on the production of biodiesel by magnetic cell biocatalyst based on lipase-producing bacillus subtilis. *Appl. Biochem. Biotechnol.* **2007**, *137*, 793–803. [[PubMed](#)]
8. Lima, L.N.; Oliveira, G.C.; Rojas, M.J. Immobilization of Pseudomonas fluorescens lipase on hydrophobic supports and application in biodiesel synthesis by transesterification of vegetable oils in solvent-free systems. *J. Ind. Microb. Biotechnol.* **2015**, *42*, 523–535. [[CrossRef](#)]
9. Amirkhani, L.; Moghaddas, J.; Jafarizadeh, H. Optimization of biodiesel production using immobilized Candida rugosa lipase on magnetic Fe₃O₄-silica aerogel. *Iran. J. Chem. Chem. Eng.* **2019**, *38*, 193–201.
10. Kalantari, M.; Yu, M.; Liu, Y.; Huang, X.; Yu, C. Engineering mesoporous silica microspheres as hyper-activation supports for continuous enzymatic biodiesel production. *Mater. Chem. Front.* **2019**, *3*, 1816–1822. [[CrossRef](#)]
11. Payá-Tormo, L.; Rodríguez-Salarichs, J. Improvement of the activity of a fungal versatile-lipase toward triglycerides: An in silico mechanistic description. *Front. Bioeng. Biotechnol.* **2019**, *7*, 71. [[CrossRef](#)] [[PubMed](#)]
12. Ramakrishna, T.R.B.; Ashton, T.D.; Marshall, S.N. Effect of Triton X-100 on the activity and selectivity of lipase immobilized on chemically reduced graphene oxides. *Langmuir* **2021**, *37*, 9202–9214. [[CrossRef](#)] [[PubMed](#)]
13. Zhang, H.; Zou, Y.; Shen, Y.; Gao, X.; Zheng, X.; Zhang, X. Dominated effect analysis of the channel size of silica support materials on the catalytic performance of immobilized lipase catalysts in the transformation of unrefined waste cooking oil to biodiesel. *BioEnerg. Res.* **2014**, *7*, 1541–1549. [[CrossRef](#)]
14. Zhang, Y.; Li, J.; Han, D.; Zhang, H.; Liu, P.; Li, C. An efficient resolution of racemic secondary alcohols on magnetically separable biocatalyst. *Biochem. Biophys. Res. Commun.* **2008**, *365*, 609–613. [[CrossRef](#)]
15. Palla, C.A.; Pacheco, C.; Carrín, M.E. Preparation and modification of chitosan particles for Rhizomucor miehei lipase immobilization. *Biochem. Eng. J.* **2011**, *55*, 199–207. [[CrossRef](#)]
16. Deng, H.T.; Wang, J.J.; Ma, M.; Liu, Z.Y.; Zheng, F. Hydrophobic surface modification of chitosan gels by stearyl for improving the activity of immobilized lipase. *Chinese Chem. Lett.* **2009**, *20*, 995–999. [[CrossRef](#)]
17. Aucoin, M.G.; Erhardt, F.A. Hyperactivation of Rhizomucor miehei lipase by hydrophobic xerogels. *Biotechnol. Bioeng.* **2004**, *85*, 647–655. [[CrossRef](#)]
18. Lu, S.; He, J.; Guo, X. Architecture and performance of mesoporous silica-lipase hybrids via non-covalent interfacial adsorption. *AIChE J.* **2009**, *56*, 506–514. [[CrossRef](#)]
19. Jin, Q.; Li, X.; Deng, C.; Zhang, Q.; Yi, D.; Wang, X. Silica nanowires with tunable hydrophobicity for lipase immobilization and biocatalytic membrane assembly. *J. Colloid Interf. Sci.* **2018**, *531*, 555–563. [[CrossRef](#)]
20. Zhang, J.; Gao, B.; Lv, K.; Kumissay, L.; Wu, B.; Chu, J. Specific immobilization of lipase on functionalized 3D printing scaffolds via enhanced hydrophobic interaction for efficient resolution of racemic 1-indanol. *Biochem. Biophys. Res. Commun.* **2021**, *546*, 111–117. [[CrossRef](#)]
21. Rodrigues, C.R.; Virgen-Ortiz, J.J.; dos Santos, C.S.J.; Berenguer-Murcia, A.; Alcántara, R.A.; Barbosa, O.; Ortiz, C.; Fernandez-Lafuente, R. Immobilization of lipases on hydrophobic supports: Immobilization mechanism, advantages, problems, and solutions. *Biotechnol. Adv.* **2019**, *37*, 746–770. [[CrossRef](#)] [[PubMed](#)]
22. Rueda, N.; dos Santos, J.C.S.; Torres, R.; Ortiz, C.; Barbosa, O.; Fernandez-Lafuente, R. Improved performance of lipases immobilized on heterofunctional octylglyoxyl agarose beads. *RSC Adv.* **2015**, *5*, 11212–11222. [[CrossRef](#)]
23. Nicolas, P.; Lassalle, V.L.; Ferreira, M.L. About the role of typical spacer/crosslinker on the design of efficient magnetic biocatalysts based on nanosized magnetite. *J. Mol. Catal. B Enzym.* **2015**, *122*, 296–304. [[CrossRef](#)]
24. Weinberger, S.; Pellis, A.; Comerford, J.W.; Farmer, T.J.; Guebitz, G.M. Efficient physisorption of candida antarctica lipase B on polypropylene beads and application for polyester synthesis. *Catalysts* **2018**, *8*, 369. [[CrossRef](#)]

25. Arana-Peña, S.; Lokha, Y.; Fernández-Lafuente, R. Immobilization of eversa lipase on octyl agarose beads and preliminary characterization of stability and activity features. *Catalysts* **2018**, *8*, 511. [CrossRef]
26. Zou, T.; Duan, Y.D.; Wang, Q.E.; Cheng, H.M. Preparation of immobilized lipase on silica clay as a potential biocatalyst on synthesis of biodiesel. *Catalysts* **2020**, *10*, 1266. [CrossRef]
27. Al-Oweini, R.; El-Rassy, H. Synthesis and characterization by FTIR spectroscopy of silica aerogels prepared using several Si (OR) (4) and R³Si (OR') (3) precursors. *J. Mol. Struct.* **2009**, *919*, 140–145. [CrossRef]
28. Urrutia, P.; Arrieta, R.; Alvarez, L.; Cardenas, C. Immobilization of lipases in hydrophobic chitosan for selective hydrolysis of fish oil: The impact of support functionalization on lipase activity, selectivity and stability. *Inter. J. Biol. Macromol.* **2018**, *108*, 674–686. [CrossRef]
29. Wang, J.; Meng, G.; Tao, K.; Feng, M.; Zhao, X.; Li, Z.; Xu, H. Immobilization of lipases on alkyl silane modified magnetic nanoparticles: Effect of alkyl chain length on enzyme activity. *PLoS ONE* **2012**, *7*, e43478. [CrossRef]
30. Machado, N.B.; Miguez, J.P.; Bolina, I.C.A.; Salviano, A.B.; Gomes, R.A.B.; Tavano, O.L.; Luiz, J.H.H.; Tardioli, P.W.; Cren, E.C. Preparation, functionalization and characterization of rice husk silica for lipase immobilization via adsorption. *Enzym. Microb. Technol.* **2018**, *128*, 9–21. [CrossRef]
31. Li, Q.; Zhai, G.Z.; Xu, Y.; Odoom-Wubah, T.; Jia, L.S.; Huang, J.L.; Sun, D.H.; Li, Q.B. Diatomite supported Pt nanoparticles as efficient catalyst for benzene removal. *Ind. Eng. Chem. Res.* **2019**, *58*, 14008–14015. [CrossRef]
32. No, D.S.; Zhao, T.T.; Lee, J.; Lee, J.S. Synthesis of phytosteryl ester containing pinolenic acid in a solvent-free system using immobilized *Candida rugosa* lipase. *J. Agr. Food Chem.* **2013**, *61*, 8934–8940. [CrossRef] [PubMed]
33. Deon, M.; Ricardi, N.C.; Andrade, R.C.D. Designing a support for lipase immobilization based on magnetic, hydrophobic, and mesoporous silica. *Langmuir* **2020**, *36*, 10147–10155. [CrossRef] [PubMed]
34. dos Santos, J.C.S.; Rueda, N.; Gonçalves, L.R.B.; Fernandez-Lafuente, R. Tuning the catalytic properties of lipases immobilized on divinylsulfone activated agarose by altering its nanoenvironment. *Enzym. Microb. Technol.* **2015**, *77*, 1–7. [CrossRef]
35. He, S.S.; Song, D.W.; Chen, M.; Cheng, H.M. Immobilization of lipases on magnetic collagen fibers and its applications for short-chain ester synthesis. *Catalysts* **2017**, *7*, 178. [CrossRef]
36. dos Santos, J.C.S.; Rueda, N.; Sanchez, A.; Villalonga, R.; Gonçalves, L.R.B.; Fernandez-Lafuente, R. Versatility of divinylsulfone supports permits the tuning of CALB properties during its immobilization. *RSC Adv.* **2015**, *5*, 35801–35810. [CrossRef]
37. Remonato, D.; de Oliveira, J.V.; Guisan, J.M.; de Oliveira, D.; Ninow, J.; Fernandez-Lorente, G. Production of FAME and FAEE via alcoholysis of sunflower oil by eversa lipases immobilized on hydrophobic supports. *Appl. Biochem. Biotechnol.* **2018**, *185*, 705–716. [CrossRef]
38. Zhang, W.W.; Yang, X.L.; Jia, J.Q.; Wang, N.; Hu, C.L. Surfactant-activated magnetic cross-linked enzyme aggregates (magnetic CLEAs) of *Thermomyces lanuginosus* lipase for biodiesel production. *J. Mol. Catalysis B Enzym.* **2015**, *115*, 83–89. [CrossRef]
39. Dong, Z.; Jiang, M.Y.; Shi, J.; Zheng, M.M.; Huang, F.H. Preparation of immobilized lipase based on hollow mesoporous silica spheres and its application in ester synthesis. *Molecules* **2019**, *24*, 395. [CrossRef]
40. GB/T 2013-2010; Density Determination Method for Liquid Petrochemical Products. Available online: <http://www.gb688.cn/bzgk/gb/newGbInfo?hcno=AE3625C61D714EBF721B10A83BA8CB93> (accessed on 8 January 2022).
41. GB/T 265-1988; Petroleum Products Kinematic Viscosity Determination Method and Dynamic Viscosity Calculation Method. Available online: <http://www.gb688.cn/bzgk/gb/newGbInfo?hcno=AD148CF5E97E23EEE5BC82FB60098519> (accessed on 8 January 2022).
42. GB 264-1983; Determination of Acid Value of Petroleum Products. Available online: <http://www.gb688.cn/bzgk/gb/newGbInfo?hcno=1CD5381B75A393C0213F549FF79016B1> (accessed on 8 January 2022).
43. GB/T 17144-1997; Determination of Residual Carbon in Petroleum Products (Micro Method). Available online: <http://www.gb688.cn/bzgk/gb/newGbInfo?hcno=CAB7C5B4326B2A08F50ECC2C7B926F77> (accessed on 8 January 2022).
44. You, Q.; Yin, X.; Zhao, Y.; Zhang, Y. Biodiesel production from jatropha oil catalyzed by immobilized *Burkholderia cepacia* lipase on modified attapulgitite. *Bioresour. Technol.* **2013**, *148*, 202–207. [CrossRef]